Combust. Sci. and Tech., 1993, Vol 91, pp. 143-161
Photocopying permitted by license only



# Finite-Rate Diffusion-Controlled Reaction in a Vortex

RONALD G. REHM, HOWARD R. BAUM, HAI C. TANG, DANIEL C. LOZIER
*National Institute of Standards and Technology Gaithersburg, MD 20899*

*(Received July 23, 1992; in final form Oct. 13, 1992)*

**ABSTRACT**—The influence of a vortex on a gaseous diffusion reaction is examined. The vortex is taken to be two dimensional, and the species are initially assumed to occupy adjacent half spaces. In the flame-sheet limit, thermal expansion and the effects of variable diffusion are taken into account. A global similarity solution exists for this problem, and a simple expression for the solution is determined in the asymptotic limit of large Schmidt number. The problem is also analyzed for finite-rate chemistry, appropriate for an isothermal, bimolecular reaction. The problem depends upon three parameters, Reynolds number, Schmidt number and the equivalence ratio, with the Damköhler number equal to the dimensionless time. The structure of the reaction region normal to the flame front is examined as a function of time. The evolution of the reaction to a state relation, dependent only upon the mixture-fraction variable, is demonstrated as the Damköhler number becomes large.

## 1 INTRODUCTION

Investigation of turbulent combustion has become an area of greatly increased activity over the past several years. This activity has occurred because both theoretical and experimental progress has been made in understanding the governing processes and also because of the great technological importance of turbulent combustion, see Williams (1985a), Williams (1985b) and the references therein.

Experiments in shear layers, starting with Brown and Roshko (1974) and including Mungal and Dimotakis (1984a), Hermanson et al. (1987) and Mungal and Frieler (1984b), for example, have demonstrated that large-scale coherent structures determine the width of the shear layer, but that intimate mixing of the different species and reaction takes place at much smaller length scales. The model of Broadwell and Breidenthal (1982), which relies upon results of many of these experiments and which has been used as the basis for interpretation of these and subsequent experiments, is based upon the concept that lateral growth of the shear layer is governed by fluid-dynamical entrainment. The fluid from the two streams in the shear layer is mechanically mixed by the cascading process often associated with turbulence to smaller and smaller length (and time) scales until it finally reaches scales at which diffusion (mass, momentum or energy) become important. Since these diffusion scales are very much smaller than the entrainment scales, the entrainment, or mechanical mixing scales are governed by very different dynamical processes than those governing the small scales at which diffusion (and in the reacting case, the reaction) take place. Subsequent examination of shear layers has involved extensive computations, see Rogallo and Moin (1984), Ghoniem et al. (1988) and Son et al. (1991) and the references therein. These computations have also verified the basic concept described above concerning the separation of scales, and have studied in detail features of the shear layers including aspects of reaction in these layers.

Likewise, experiments in fire research, in which buoyant convection as opposed to forced convection is essential, indicate that, when the Grashof number (which is proportional to the Reynolds number squared) is large, the length and time scales associated with turbulent combustion can also be separated and analyzed differently. At the largest length scales, the geometry defines the flow field, which is essentially inviscid or nondissipative away from boundaries. At smaller scales, where the combustion occurs, diffusion of the fuel and oxidizer into each other and reaction takes place, with subsequent reactant

consumption and heat release. Finally, at still smaller scales, the structure of the reaction zone in individual flamelets is important and chemical species concentrations can be determined. The essence of the model of fire-induced turbulent combustion outlined in Baum et al. (1989) is to analyze each of these three scales and to couple them through their dynamical interactions.

Marble (1985) proposed a two dimensional model problem of small-scale mixing and reaction, which he and his colleagues studied extensively through analytical means Karagozian and Marble (1986a), Karagozian (1982), Karagozian and Manda (1986b) and Norton (1983). The model is important because it includes the two-dimensional effects of flame stretching and convective enhancement of diffusion in a diffusion-controlled reaction in a viscously spreading vortex. The analytical method utilized by Marble to attack this problem is based on a technique developed earlier by Carrier, Fendell and Marble (1975) in which the flame front is analyzed locally, assuming that the front is sharp, and summing over this flame front to obtain global dependences of consumption rates upon the governing parameters.

There are several limitations of the model and the analysis utilized by Marble and coworkers, some apparent and others tacit. The original model proposed by Marble (1985) is based on an isothermal or constant-density model for the reaction, a very common, but limiting assumption for combustion. The analysis, while intuitive, clever and correct under many conditions, does not provide the basis for determining the limits of validity for the approximations obtained. This methodology was subsequently applied by coworkers of Marble, Karagozian and Marble (1986a), Karagozian (1982), Karagozian and Manda (1986b), Norton (1983) and by others, Cetegen and Sirignano (1990), Cetegen and Bogue (1991), to both extend the model and to apply the model to other questions of interest. In Marble (1985) and Karagozian and Marble (1986a) for example, the constant-density approximation was relaxed to roughly determine the effects of thermal expansion when the chemical reaction is mildly exothermic, and in Norton (1983) and Cetegen and Bogue (1991), some effects of finite-rate chemistry were examined. Since the mathematical limitations of these analyses are not clear, Rehm et al (1989) examined this question in their analysis of the original Marble problem, noting that this problem allows a global similarity solution.

In addition to the generalizations of the methodology used by Marble to solve this problem and its extensions, other researchers have taken different tacks to obtaining solutions. Laverdant and Candel, (1988a), Laverdant and Candel (1988b), and Laverdant and Candel (1989), have used finite difference methods to examine the problem while Meiburg (1990) has used Lagrangian, vortex tracking numerical methods to examine the effects of thermal expansion and baroclinic vorticity generation on the vortex, diffusion-flame interaction. Also, Macaraeg et al (1992) have used a combination of asymptotic and numerical methods to examine the problem for finite-rate chemistry, concentrating on the initiation of the reaction. In all cases, the interest in both analytical and computational studies is to isolate particular physical effects and study these effects for the purpose of understanding and possible control of the large scale structures in combustion.

In the present paper, the authors extend the analysis presented in Rehm et al. (1989) to consider both the effects of thermal expansion on a flame-sheet analysis and the effects of finite-rate chemistry on a non-premixed flame, vortex interaction. We emphasize that, although numerical evaluations are performed to obtain results, this study is an analytical one based on the conservation equations; it is not based upon intuitive approximations, but introduces approximations whose validity can be ascertained. The context of the work is unwanted fires, the primary area of interest of the authors. In unwanted fires, it is generally expected that fuel enters the gaseous state from either a solid or a liquid phase through pyrolization or evaporation by heat transfer from existing flames; hence

the ignition of the fire is assumed and only the enhancement of the ongoing combustion rate by mixing is of concern. Therefore, in contrast to the analysis on finite-rate effects of Macaraeg et al. (1992), we do not examine the initiation process, but rather the transition of the finite-rate process over to the flame-sheet limit. Also, in contrast to the intuitive nature of the analysis methods used in Norton (1983) and Cetegen and Sirignano (1990), we utilize an analytical approach starting from the conservation equations, similar to our earlier methods Rehm et al. (1989).

In Section 2 we formulate the problem allowing for heat release and thermal variation of the transport properties. In Section 3 the case of infinite-rate chemistry is considered including heat release and variable transport properties, and an asymptotic solution valid for large Schmidt number is presented. This solution is new and quite simple. In Section 4 we analyze the problem when there is a time scale associated with the combustion chemistry; for this analysis, we assume constant-temperature finite-rate chemistry. The consequences of the analysis are compared with the infinite-rate case. In Section 5, results are presented, and conclusions are given in Section 6.

## 2 FORMULATION OF THE PROBLEM

Consider the problem in which initially there is fuel in the left half-plane and oxidizer in the right half-plane in arbitrary proportions specified by the initial equivalence ratio. These half-spaces are brought into contact and simultaneously a line vortex with axis at the origin is imposed (see Fig. 1). The vortex induces a convective mixing of the interface between the two species, increasing the area of the separating surface in the neighborhood of the origin and enhancing the diffusion of the species into each other. For these conditions, the general equations are:
The species equations:

$$\rho\left(\frac{\partial Y_i}{\partial t} + \vec{u}\cdot\nabla Y_i\right) = \nabla\cdot(\rho D_i \nabla Y_i) + W_i \tag{1}$$

The energy equation:

$$\rho\left(\frac{\partial C_p T}{\partial t} + \vec{u}\cdot\nabla C_p T\right) = \nabla\cdot(\rho C_p k \nabla T) + \dot{q} \tag{2}$$

The continuity equation:

$$\frac{\partial \rho}{\partial t} + \nabla\cdot(\rho\vec{u}) = 0 \tag{3}$$

The state equation:

$$p = \rho R T \tag{4}$$

In these equations, symbols have their usual meanings: $Y_i$ are the mass fractions of $i = 1 = f$ fuel, $i = 2 = o$ oxidizer and $i = 3 = p$ product; $\rho$ is density, $\vec{u}$ is the velocity, $D_i$ are the diffusivities, $W_i$ are the reaction rates, $T$ is temperature, $C_p$ is the constant-pressure specific heat, $k$ is the thermal diffusivity, $\dot{q}$ is the reaction heat release rate, $p$ is the pressure and $R$ is the gas constant. These equations are supplemented by the Navier-Stokes equations representing momentum conservation.

## 3 FLAME-SHEET PROBLEM

### *3.1 Pseudo-Mixture Fraction Variable*

In this subsection, we consider a general formulation for the flame-sheet approximation which allows the fluid to expand with the heat released by the reaction and also takes

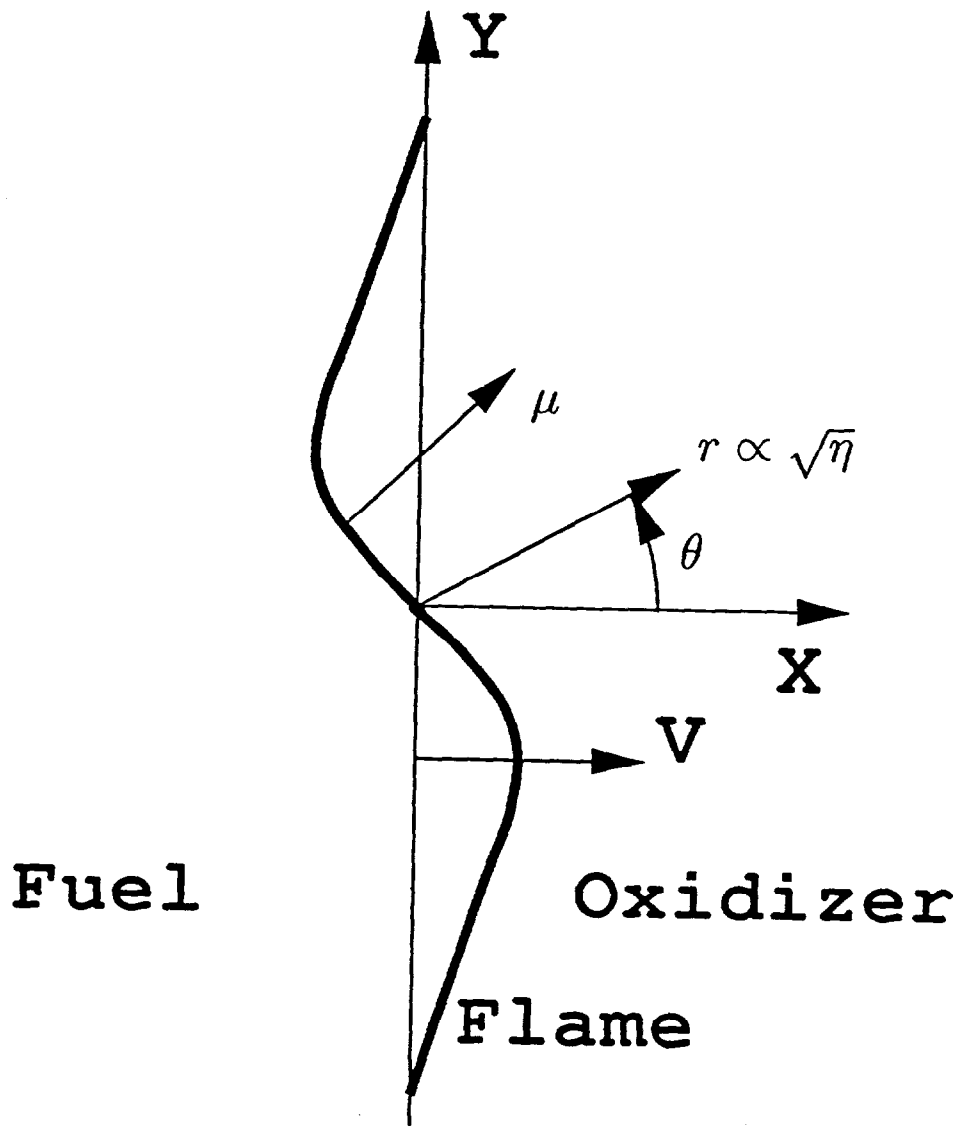


FIGURE 1 Schematic diagram of vortex, flame-sheet interaction, showing fuel on the left, oxidizer on the right and some of the independent variables used in the analysis.

account of variable transport properties. This analysis follows very closely that of Baum et al. (1991) and is presented in abbreviated form for completeness; for more information on the pseudo-mixture fraction formulation, see Baum et al. (1991). In this model, we define a Shvab-Zeldovich or mixture-fraction variable

$$\tilde{Z} = \frac{Y_f/v_f M_f - Y_o/v_o M_o + Y_{oo}/v_o M_o}{Y_{fo}/v_f M_f + Y_{oo}/v_o M_o} \tag{5}$$

for which a linear combination of Eqs. (1) yields, assuming all diffusion coefficients to be equal,

$$\rho\left(\frac{\partial \tilde{Z}}{\partial t}+\vec{u}\cdot\nabla\tilde{Z}\right)=\nabla\cdot(\rho D\nabla\tilde{Z}) \tag{6}$$

Here, the $v_i$ are the stoichiometric coefficients, the $M_i$ are the molecular weights, and the subscripts $f, o$ represent fuel and oxidizer respectively. The initial and boundary conditions for $\tilde{Z}$ are $\tilde{Z}=1$ for $x<0$ and $\tilde{Z}=0$ for $x>0$.

We now assume that (see Baum et al. (1991) for a more general discussion) all thermodynamic and transport properties can be related uniquely to $\tilde{Z}$ through a library of state relationships, and split the velocity field into a solenoidal component and an irrotational component, as follows:

$$\vec{u}=\vec{v}+\nabla\phi \tag{7}$$

where $\nabla\cdot\vec{v}=0$ and $\nabla\times\vec{v}=\vec{\omega}$. Then, the vector potential for the irrotational velocity component satisfies the equation:

$$\nabla^2\phi=-\frac{1}{\rho^2}\frac{d\rho}{d\tilde{Z}}\nabla\cdot(\rho D\nabla\tilde{Z}) \tag{8}$$

which is obtained by manipulating the continuity equation, Eq. (3) and the mixture-fraction equation, Eq. (6).

Define

$$F(\tilde{Z})\equiv\frac{\int_0^{\tilde{Z}}\rho(z)D(z)dz}{\int_0^1\rho(z)D(z)dz} \tag{9}$$

Then

$$\nabla^2\phi=-\frac{1}{\rho^2}\frac{d\rho}{d\tilde{Z}}\int_0^1\rho(z)D(z)dz\,\nabla^2F \tag{10}$$

We assume that the state relationship can be reasonably approximated by Baum et al. (1991): $-\frac{1}{\rho^2}\frac{d\rho}{d\tilde{Z}}=\frac{dV}{d\tilde{Z}}=$ constant. Then

$$\nabla^2\phi=\mp K_\pm\nabla^2F \tag{11}$$

where the upper sign is for $0\le\tilde{Z}\le\tilde{Z}_s$ and the lower sign is for $\tilde{Z}_s\le\tilde{Z}\le 1$. Here, the subscript $s$ stands for the flame sheet. Define $Z(\tilde{Z})$ as follows:

$$Z=a_\pm+b_\pm\exp(\mp K_\pm F/D_s) \tag{12}$$

where the upper sign is for $0\le F\le F_s$ and the lower sign is for $F_s\le F\le 1$. We require that

$$Z(F_s+)=Z(F_s-)$$

$$\frac{\partial Z}{\partial n})_{s+}=\frac{\partial z}{\partial n})_{s-}$$

and these requirements determine the constants $a_\pm$ and $b_\pm$ (see Baum et al. (1991)).

$$a_+=b_-(K_-/K_+)\exp[F_s(K_++K_-)/D_s]=b_+$$

$$a_- = 1 - b_- \exp(K_-/D_s)$$

$$b_- = [(\exp(K_-/D_s) - \exp(K_-F_s/D_s)$$

$$+(K_-/K_+)\exp[(K_- + K_+)F_s/D_s][1 - \exp(-K_+F_s/D_s)]]^{-1} \tag{13}$$

$Z$ is the pseudo-mixture-fraction and at large Reynolds numbers satisfies the constant-property convection-diffusion equation often analyzed for the mixture-fraction variable.

$$\frac{\partial Z}{\partial t} + \vec{u} \cdot \nabla Z = D_s \nabla^2 Z \tag{14}$$

Here, the initial conditions (I.C.) are $Z = 1$ for $x < 0$ and $Z = 0$ for $x > 0$. $D_s$ is the value of the diffusion coefficient at the flame sheet (at the flame temperature), see Baum et al. (1991) for more discussion.

The pseudo-mixture-fraction variable allows us immediately to interpret all of the analysis of the flame-sheet problem for the mixture-fraction variable in a fluid with constant properties more generally in terms of a flame-sheet model which includes both thermal expansion from reaction and transport properties depending upon temperature and density. In particular, each contour for a constant value of the pseudo-mixture-fraction $Z$ represents a flame-sheet location for a specific value of the equivalence ratio, and the transformations given by Eqs. (9) and (12) determine how each flame sheet is moved relative to the origin where the vortex is located by thermal effects. In addition, the irrotational component of the velocity resulting from thermal expansion and variable transport properties is determined from the vector potential given in Eq. (8) once the mixture-fraction variable has been found, as it is approximately for large Schmidt numbers in the following subsection.

### *3.2 Large-Schmidt Number Asymptotic Solution*

In this section, we examine the Marble problem using the pseudo-mixture-fraction formulation presented above and obtain a quite simple asymptotic solution valid for large Schmidt numbers. This solution is new and simplifies considerably the solution of the more general problem where one is interested in the effects of finite-rate chemistry.

At this point we specialize to the Marble problem, specifying the tangential velocity $v_\theta$ imposed as

$$v_\theta(r,t) = r\frac{d\theta}{dt} = \frac{\Gamma}{2\pi r}[1 - \exp(-\eta)] \tag{15}$$

where $\Gamma$ is the circulation of the vortex, $\nu$ is the kinematic viscosity and $\eta = r^2/4\nu t$ is a similarity variable. This velocity field satisfies the Navier-Stokes equations, and is the solenoidal portion of the velocity field utilized in the analysis above. The equation for the pseudo-mixture-fraction variable is then

$$\frac{\partial Z}{\partial t} + \frac{v_\theta}{r}\frac{\partial Z}{\partial \theta} - D_s\left(\frac{\partial^2 Z}{\partial r^2} + \frac{1}{r}\frac{\partial Z}{\partial r} + \frac{1}{r^2}\frac{\partial^2 Z}{\partial \theta^2}\right) = 0 \tag{16}$$

The problem is made dimensionless using the kinetics time scale $\tau_0 = \nu_o M_o/\tilde{k}\,Y_{o0}$, the length scale defined by this time and the diffusion coefficient $l = \sqrt{D_s \nu_o M_o/\tilde{k}\,Y_{o0}}$ and the concentrations with respect to their initial values. Here, $\tilde{k}$ is the value of the kinetics rate coefficient at the flame temperature. With this scaling, the dimensionless time becomes a Damköhler number. Three dimensionless parameters enter the problem,

the equivalence ratio, $\alpha \equiv Y_{fo}\nu_o M_o / Y_{oo}\nu_f M_f$, the Schmidt number, $Sc \equiv \nu/D$, and the Reynolds number, $Re \equiv \Gamma/(4\pi\nu)$. First, the similarity variable becomes

$$\eta = r^2/(4Sc_t) \tag{17}$$

while equation (15) becomes

$$v_\theta(r,t) = r\,d\theta/dt = (2ReSc/r)[1 - \exp(-\eta)] \tag{18}$$

As in Rehm et al. (1989) we change to Lagrangian coordinates. Integrating the tangential velocity gives the angle $\theta(r, \theta_0, t)$ at time $t$ for any fluid element initially located at $r, \theta_0$. A change of variables to the Lagrangian coordinates, $r_o, \theta_o, \tau$,

$$\begin{aligned} r &= r_0 \\ \theta &= \theta_o + \frac{Re}{2}\frac{1 - E_2(\eta)}{\eta} \\ t &= r \end{aligned} \tag{19}$$

where $E_j(z) = \int_1^\infty t^{-j}\exp(-zt)dt$, can then be made in all of the equations. For the problem posed above for the mixture-fraction variable (which we call the Marble problem), there are no length or time scales, and we find that $Z$ is only a function of the similarity variable $\eta$ and the angle $\theta_0$.

The use of Lagrangian coordinates eliminates the need to resolve small-scale internal transition layers which arise when the Reynolds number is large. With this transformation the problem reduces simply to a time-dependent diffusion problem. The equation for the mixture fraction in Lagrangian variables becomes:

$$\begin{aligned} &\frac{\partial Z}{\partial \tau} - \left(\frac{\partial^2 Z}{\partial r_0^2} + \frac{1}{r_0}\frac{\partial Z}{\partial r_0} + \left[\left(Re\frac{1 - e^{-\eta}}{\eta}\right)^2 + 1\right]\frac{1}{r_0^2}\frac{\partial^2 Z}{\partial \theta_0^2}\right) \\ &- \left(\frac{2Re}{r_0^2}\left(e^{-\eta} - \frac{1 - e^{-\eta}}{\eta}\right)\frac{\partial Z}{\partial \theta_0} + \frac{Re}{r_0}\frac{1 - e^{-\eta}}{\eta}\frac{\partial^2 Z}{\partial r_0 \partial \theta_0}\right) = 0 \end{aligned} \tag{20}$$

The solution depends *only* upon the similarity variable and angle.

In Rehm et al. (1989) the Marble problem was solved by Fourier analyzing the mixture fraction variable in the Lagrangian angle $\theta_0$, solving the linear, two-point boundary value problem by asymptotic and numerical methods, and Fourier synthesizing the complete solution. The asymptotic analysis involved a large-Schmidt-number approximation. The applicability of this approximation was tested against the direct numerical solution of the equations, and the conclusion was that the large-Schmidt-number approximation has wider applicability than one might initially expect. Recent experimental evidence of Dahm and Buch (1989) comparing mixing in liquids and gases confirms the conclusion that a large-Schmidt-number approximation, which is definitely valid in liquids, is qualitatively (and approximately quantitatively) valid also in gases.

In this section a new, much simpler asymptotic solution is derived for the mixture fraction when the Schmidt number is large. The asymptotic results compare well with those obtained in Rehm et al. (1989) over ranges of interest. The method used to obtain the mixture fraction is then utilized in the following section on the more general problem with finite-rate kinetics. It is convenient to use the similarity variable, $\eta = r_0^2/(4Sc\tau)$, and the Lagrangian coordinate normal to the interface between the fuel and the oxidizer,

$\varsigma = \sqrt{Sc\eta}\cos\theta_0$. The resulting equation for the mixture fraction is messy and is not stated here, see Rehm et al. (1992). However, this equation simplifies considerably and allows additional analysis when the Schmidt number is large. For large Schmidt numbers and for $\eta > 0$, Eq. (20) becomes

$$\eta\frac{\partial Z}{\partial \eta} + \frac{\varsigma}{2}\frac{\partial Z}{\partial \varsigma} + \frac{1}{4}\left[\left(Re\frac{1-e^{-\eta}}{\eta}\right)^2 + 1\right]\frac{\partial^2 Z}{\partial \varsigma^2} = 0 \tag{21}$$

where $Z \to 1$ as $\varsigma \to -\infty$ and $Z \to 0$ as $\varsigma \to \infty$.

We now make a final change in variables from $\varsigma$ to $\mu$

$$\mu = \varsigma f(\eta) \tag{22}$$

where

$$f(\eta) = \frac{1}{\sqrt{1 + Re^2 f_1(\eta)}}$$

$$f_1(\eta) = [1/3 - 2E_4(\eta) + E_4(2\eta)]/\eta^2 \tag{23}$$

$$E_j(x) = \int_1^\infty t^{-j}\exp(-xt)dt$$

Function $f_1(\eta)$ was introduced in Rehm et al. (1989), where its properties were discussed.

With this new independent variable, and assuming that $Z$ only depends on $\mu$, Eq. (21) becomes

$$2\mu\frac{\partial Z}{\partial \mu} + \frac{\partial^2 Z}{\partial \mu^2} = 0 \tag{24}$$

and this equation has solution

$$Z(\mu) = (1/2)\mathrm{erfc}(\mu) \tag{25}$$

satisfying boundary conditions that $Z \to 1$ as $\mu \to -\infty$ and $Z \to 0$ as $\mu \to \infty$. This corresponds to boundary conditions in Eq. (21) stated in terms of $\eta$ and $\zeta$. It should be noted that the error function profile for $Z$, which also emerges in the approximate analyses noted above, is here derived in terms of the asymptotically exact independent variable. This is *not* the variable which emerges from more approximate analyses.

## 4 FINITE-RATE CHEMISTRY PROBLEM

For the problem of finite-rate combustion, we assume a single-step reaction

$$\nu_f[Y_f] + \nu_o[Y_o] \to \nu_p[Y_p]$$

and that the reaction rate does not depend upon temperature, i.e., that there has been ignition and that the reaction is bimolecular. With these assumptions together with the assumptions described above, the species equations are decoupled also from the continuity equation. For analysis of the effects of finite rate of reaction, we now abandon the thermally expandable fluid with variable-property transport coefficients; the fluid has constant density.

$$\frac{\partial Y_i}{\partial t} + \frac{v_\theta}{r}\frac{\partial Y_i}{\partial \theta} - D\left(\frac{\partial^2 Y_i}{\partial r^2} + \frac{1}{r}\frac{\partial Y_i}{\partial r} + \frac{1}{r^2}\frac{\partial^2 Y_i}{\partial \theta^2}\right) = -\tilde{k}Y_f Y_o \tag{26}$$

where $i = 1, 2$ and $D$ are the species diffusion coefficients, assumed to be constant and equal. The initial conditions are that $Y_f = Y_{f0}, Y_o = 0$ for $\pi/2 \leq \theta \leq 3\pi/2$ and $Y_f = 0, Y_o = Y_{o0}$ for $-\pi/2 \leq \theta \leq \pi/2$.

Rather than solve directly Eqs. (26), we introduce another dependent variable, in addition to the mixture-fraction variable, the difference between one species concentration and the mixture-fraction variable. Using the mixture fraction variable $Z$, we can eliminate the oxidizer concentration from the equations

$$\frac{Y_o}{\nu_o M_o} = \frac{Y_f}{\nu_f M_f} + \frac{Y_{oo}}{\nu_o M_o} - \left(\frac{Y_{fo}}{\nu_f M_f} + \frac{Y_{oo}}{\nu_o M_o}\right) Z$$

$$Y_o / Y_{o0} = \alpha W + 1 - Z \tag{27}$$

Then the equation for the $Y_f$ has the same left side as before while the right side is $-\tilde{k} Y_f((Y_f/\nu_f M_f) + (Y_{oo}/\nu_o M_o) - [(Y_{fo}/\nu_f M_f) + (Y_{oo}\nu_f M_f)]Z$. We then change the dependent variable from $Y_f$ to $W$.

$$W(r_o, \theta_o, \tau) = Y_f(r_o, \theta_o, \tau)/Y_{f0} - Z(\eta, \theta_o) \tag{28}$$

The initial conditions are that $W = 0$ at $t = 0$, and the boundary conditions are that $W \to 0$ as $r \cos\theta \to \pm\infty$ away from $\theta = \pm\pi/2$.

The equation for $W$ becomes

$$\frac{\partial W}{\partial t} + \frac{v_\theta}{r}\frac{\partial W}{\partial \theta} - \left(\frac{\partial^2 W}{\partial r^2} + \frac{1}{r}\frac{\partial W}{\partial r} + \frac{1}{r^2}\frac{\partial^2 W}{\partial \theta^2}\right) \tag{29}$$

$$= -(W + Z)(\alpha W + 1 - Z)$$

where all variables are dimensionless.

### 4.1 *Solution to Finite-Rate Problem*

Changing variables from Eulerian to Lagrangian in Eq. (29) yields

$$\frac{\partial W}{\partial r} - \left(\frac{\partial^2 W}{\partial r_0^2} + \frac{1}{r_0}\frac{\partial W}{\partial r_0} + \left(\left(Re\frac{1 - e^{-\eta}}{\eta}\right)^2 + 1\right)\frac{1}{r_0^2}\frac{\partial^2 W}{\partial \theta_0^2}\right)$$

$$- \left[\frac{2Re}{r_0^2}\left(e^{-\eta} - \frac{1 - e^{-\eta}}{\eta}\right)\frac{\partial W}{\partial \theta_0} + \frac{2Re}{r_0}\frac{1 - e^{-\eta}}{\eta}\frac{\partial^2 W}{\partial r_0 \partial \theta_0}\right] \tag{30}$$

$$= -[W + Z][\alpha W + 1 - Z]$$

with initial conditions that $W = 0$ at $\tau = 0$ and boundary conditions that $W \to 0$ as $r_0 \cos(\theta_0) \to \pm\infty$ for $\theta_0$ away from $\pm\pi/2$.

Again we change to the the similarity variable, $\eta = r_0^2/(4Sc\tau)$, and the Lagrangian coordinate normal to the interface between the fuel and the oxidizer, $\varsigma = \sqrt{Sc\eta}\cos\theta_0$. For large Schmidt number (to leading order in $Sc$), the equation for the dimensionless species concentration becomes, for $\eta > 0$,

$$\tau\frac{\partial W}{\partial \tau} - \eta\frac{\partial W}{\partial \eta} - \frac{\varsigma}{2}\frac{\partial W}{\partial \varsigma} - \frac{1}{4}\left[\left(Re\frac{1 - e^{-\eta}}{\eta}\right)^2 + 1\right]\frac{\partial^2 W}{\partial \varsigma^2} \tag{31}$$

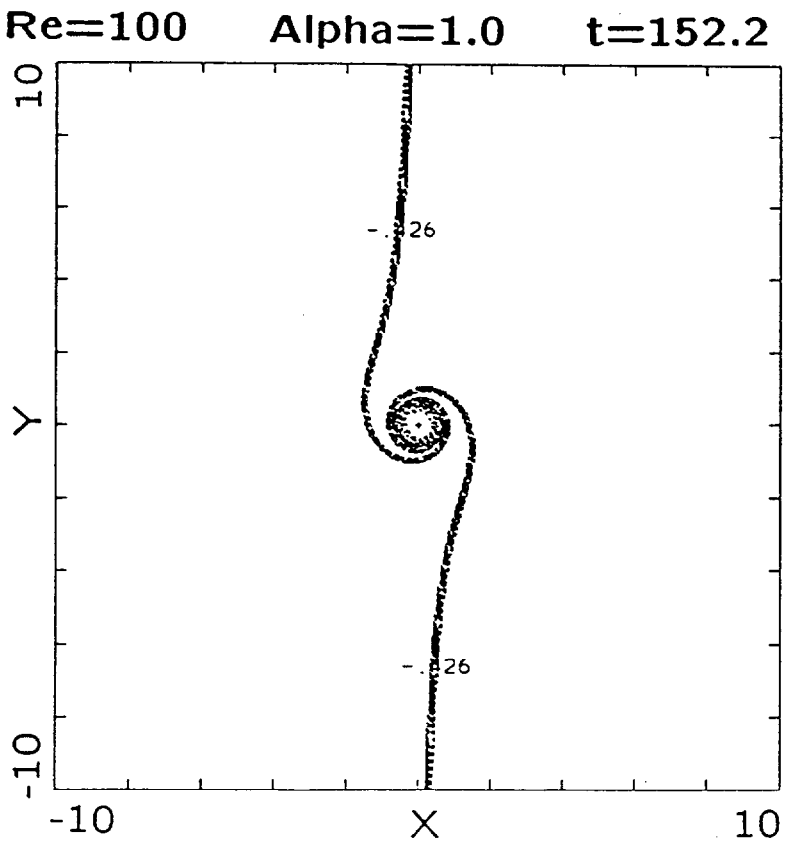


FIGURE 2 (a) Plot of the variable $W$ at time $t' = 152$ for the parameters $Re = 100, Sc = 10$ and $\alpha = 1$. $W$ is defined as the dimensionless difference between species 1 and the mixture-fraction variable (see Eq.(28).

$$= -\tau(W + Z)(\alpha W + 1 - Z)$$

where the boundary conditions are that $W \to 0$ as $\varsigma \to \pm\infty$.

With a change of variables to $\mu, \eta' = \eta/\tau$ and $\tau = t$, Eq. (31) becomes

$$t\frac{\partial W}{\partial t} - \frac{1}{4}F(\eta'/t)(2\mu\frac{\partial W}{\partial \mu} + \frac{\partial^2 W}{\partial \mu^2}) = -t[W + Z(\mu)][\alpha W + 1 - Z(\mu)] \qquad (32)$$

where

$$F(\eta) = \left[\left(Re\frac{1 - \exp(-\eta)}{\eta}\right)^2 + 1\right] f^2(\eta) \qquad (33)$$

and where $W \to 0$ as $\mu \to \pm\infty$.

We now discuss some of the properties of Eq. (32). Note again that the dimensionless time is a Damköhler number (the ratio of a residence time for diffusion to the chemical reaction time). First, away from the reaction zone (i.e., for $\eta'$ and $\mu$ not too small and for $t$ not too large), the right side must be zero. Setting this term, the chemical reaction term, to zero implies either that $W + Z(\mu)$ or $\alpha W + 1 - Z(\mu)$ is zero. If the first term

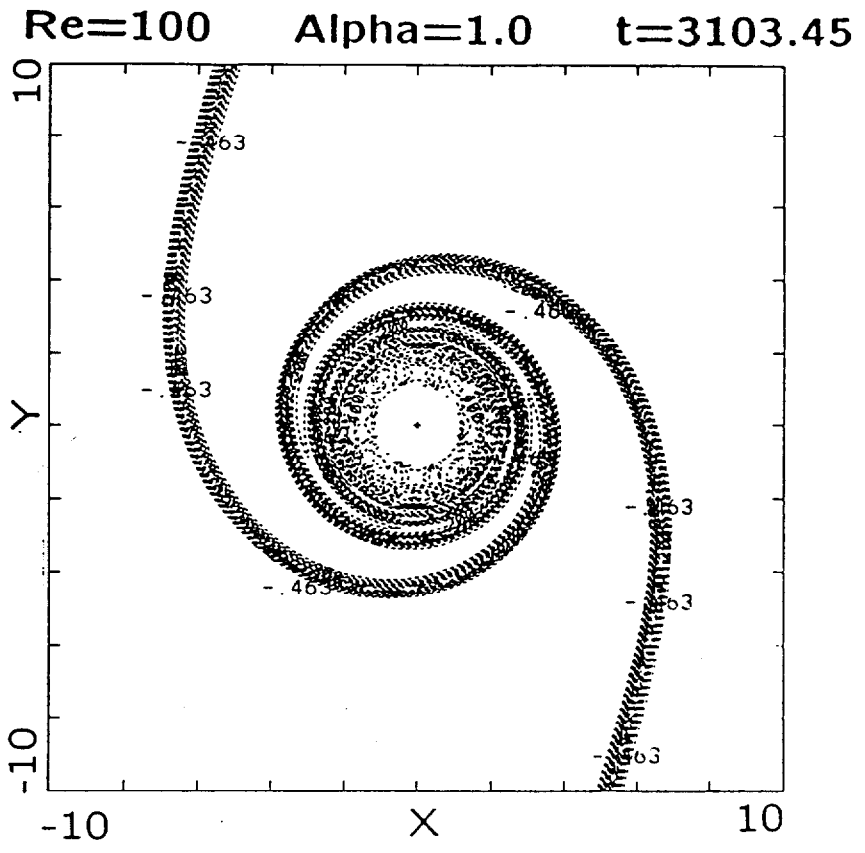


FIGURE 2 (b) Plot of the variable $W$ at time $t' = 3103$ for the parameters $Re = 100, Sc = 10$ and $\alpha = 1$. $W$ is defined as the dimensionless difference between species 1 and the mixture-fraction variable (see Eq.(28).

is zero, both $W$ and $Z$ are zero, and therefore, we are in the region where there is all fuel (and no reaction). Similarly, if the second term is zero, both $W$ and $1-Z$ are zero, and we are in the region where there is all oxidizer (and no reaction). Also, for large $\eta'$ or small $t$, and any $\mu$, the equation reduces to that of the one-dimensional (1-D) version the problem (the diffusion-reaction problem with no vortex field).

We have formulated this 1-D problem as two coupled equations, one for the mixture fraction and the second for the dimensionless species concentration, and we have utilized the fact that a similarity solution exists for the case of infinite-rate chemistry. When the 1-D problem is formulated in this fashion, Eq. (32) is obtained with $F(\eta) \equiv 1, \mu = \varsigma = x/(2\sqrt{Sct})$ and $x, t$ the dimensionless distance and time, with $Sc \equiv 1$. The important point to note is that the two-dimensional problem reduces to the one-dimensional case when either the Reynolds number is zero or at large distances from the vortex center where the imposed velocity vanishes, i.e., when the function $F(\eta'/t)$ is approximately unity. The 1-D equation is a good approximation to the full 2-D problem even for large Re provided that the time is small and radius not too small.

This one-dimensional problem has been formulated earlier and solved by asymptotic methods by Kapila (1983), who formulated the problem as two coupled equations for the dimensionless species concentrations. He determined asymptotically the properties

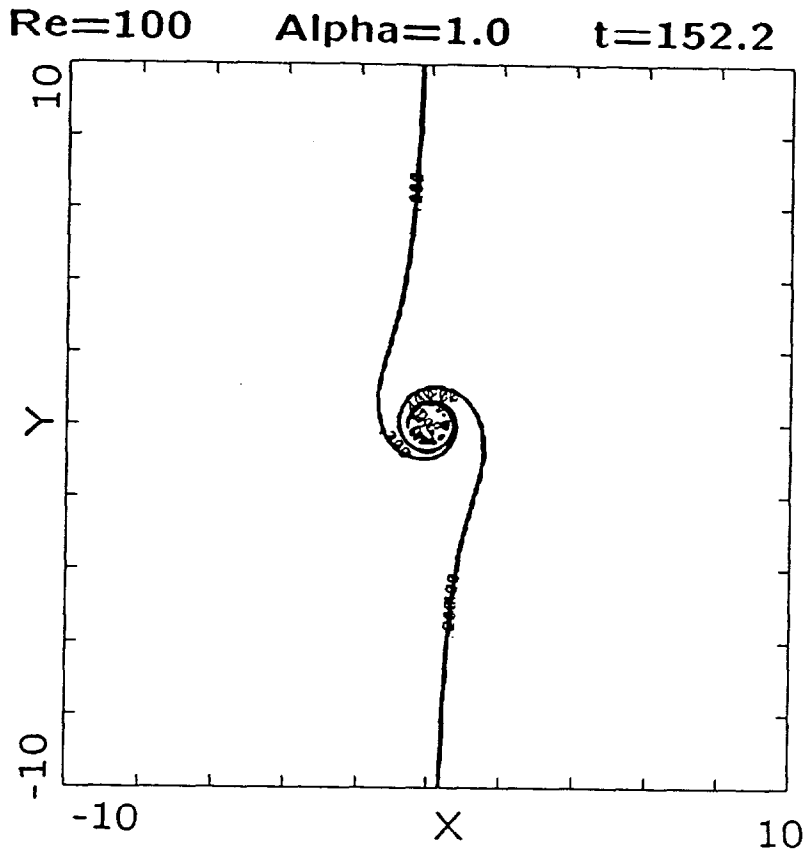


FIGURE 3 (a) Plot of the mixture-fraction variable $Z$ at time $t' = 152$ for the parameters $Re = 100$, $Sc = 10$ and $\alpha = 1$.

of the problem both at early and late dimensionless times and determined the structure of the flame sheet as time becomes large. All of these results apply directly to the 2-D problem away from the imposed vortex where $F(\eta) \approx 1$. Each species is initially a step function with all fuel to the left of the interface and all oxidizer to the right. At early times, each diffuses according to the 1-D solution to the diffusion equation for an initial step function, namely, according to the well-known complementary error function solution. Later, there are outer regions where the fuel and oxidizer remain undisturbed and the reaction is still zero, separated by the region where the fuel and the oxidizer make the transition from their undisturbed values to zero. Imbedded in this transition region is the flame structure, determined by a full transient reaction-diffusion balance that can be cast as a problem reported earlier in the literature, Friedlander and Keller (1963). It should be noted that the flame structure cannot be evaluated by analytical means, but requires numerical evaluation. Therefore, we have chosen to determine the solution to Eq. (32) directly by numerical methods, and these results are presented in the last section.

For early times, however, Eqs. (32) and (33) simplify considerably allowing an approximate solution in terms of special functions Rehm et al. (1992). At late times, results can be related Rehm et al. (1992) to those obtained by Kapila. Also, the

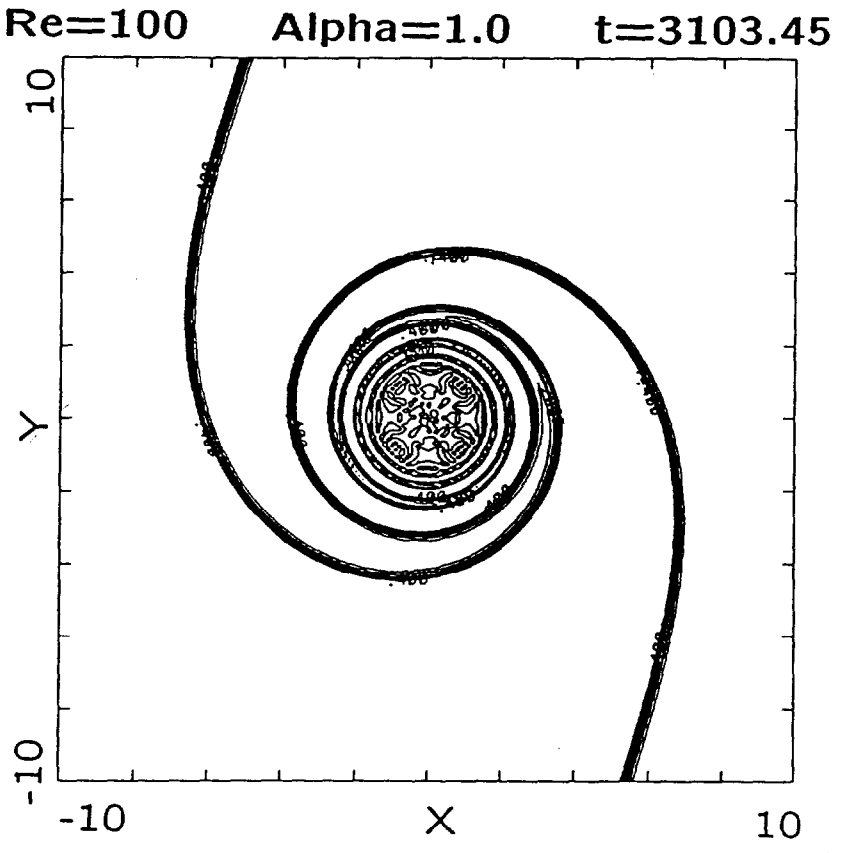


FIGURE 3 (b) Plot of the mixture-fraction variable $Z$ at time $t' = 3103$ for the parameters $Re = 100, Sc = 10$ and $\alpha = 1$.

expressions derived above can be used to obtain expressions for the consumption rate, which is proportional to time at early times and constant at late times Rehm et al. (1992).

## 5 RESULTS

We now show spatial and temporal results for $Re = 100, Sc = 10$, and $\alpha = 1$. In Fig. 2, two plots of contours of $W$ are shown at dimensionless times $t' = 152$ and 3103 as computed from Eq. (32). The contours are generated in the $\eta$ plane and plotted by evaluating $W$ on a 10 unit by 10 unit grid using NCAR graphics. The numbers on the plots designate maximum contour levels; the specific values are not important. What is important is the overall temporal and spatial behavior of the solution, which can be ascertained from this figure and the following two. The deviation of the species from that found using flame-sheet analysis, $W$, is found to change from its initial value, zero, to its minimum value, -0.5, as a spiral that slowly winds up and expands out into the plane, indicating how the structure of the combustion zone changes in physical space as time progresses. It should be noted that in the core of the expanding spiral region, the value of $W$ becomes zero again because the reaction is complete. As noted in the last

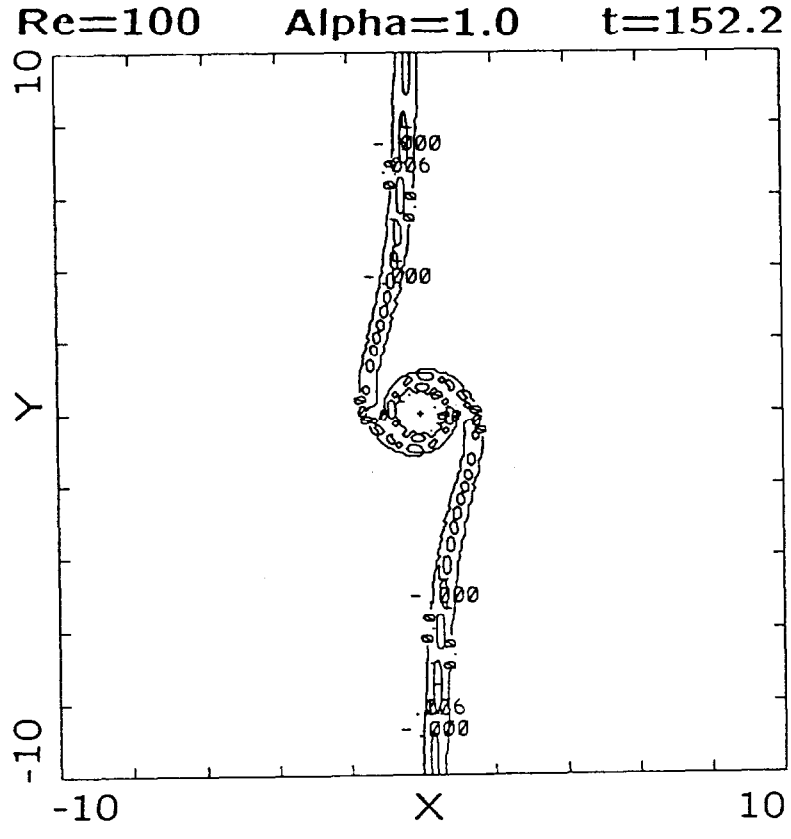


FIGURE 4 (a) Plot of the reaction rate at time $t' = 152$ for the parameters $Re = 100, Sc = 10$ and $\alpha = 1$.

section, for early times, there is only a reaction-diffusion balance; convection has not had time to develop and to distort this balance. For the scale used here, this balance is the appropriate one everywhere except near the origin. Therefore, even up to a few units of time, $W$ is essentially zero everywhere except along the vertical axis and within about a unit of the origin, where only slight rotational distortion has begun to occur.

Contours of $Z$, the mixture-fraction variable, are shown in Figure 3 for the same two times as in the preceding figure. These plots appear qualitatively similar to those shown in Fig. 2. Again, the numbers on the plots, indicating the relative contour levels, can be ignored. It should be noted, however, that each contour of constant mixture fraction $Z$ represents a flame sheet for a different value of the equivalence ratio ($\alpha = Y_{fo}\nu_o M_o / Y_{oo}\nu_f M_f$). For unit stoichiometry the flame sheet remains along the $y$-axis far from the origin; for other values of the equivalence ratio, the flame sheet either follows a contour on the fuel-rich side ($1/2 \leq Z \leq 1$) or on the fuel-lean side ($0 \leq Z \leq 1/2$).

Plots of the reaction rate at these times are shown in Figure 4 and are also qualitatively similar to those shown in Figs. 2 and 3. However, the reaction takes place in such a narrow region, that most of the contours shown in Fig. 4 are zero, and the plotting package does not perform very well in illustrating the behaviour of this quantity. (Obtaining clear and

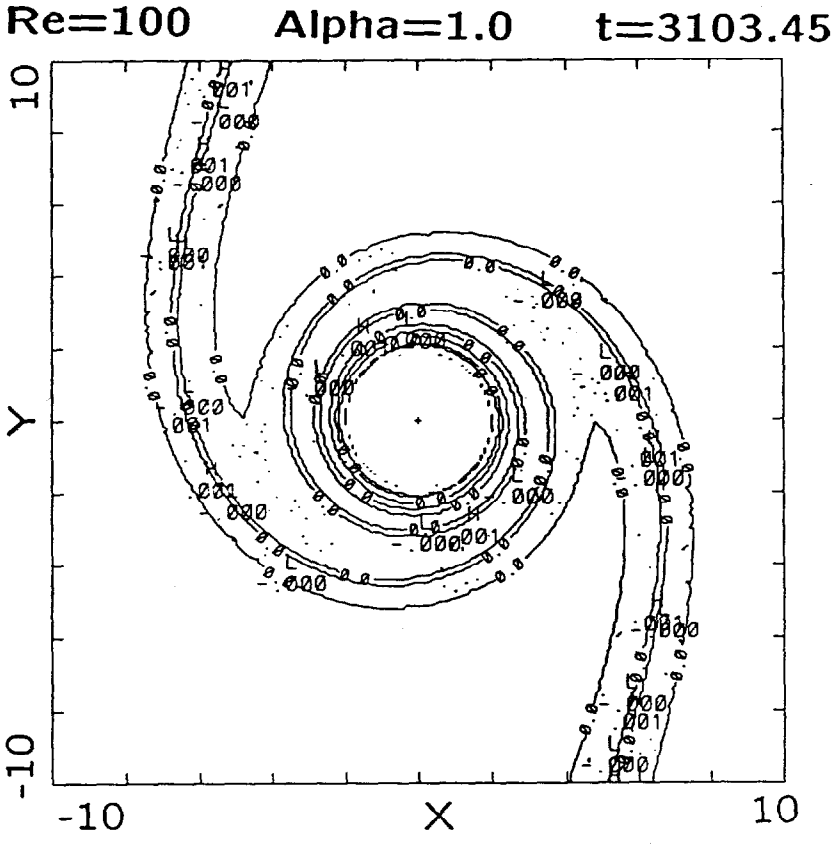


FIGURE 4 (b) Plot of the reaction rate at time $t' = 3103$ for the parameters $Re = 100, Sc = 10$ and $\alpha = 1$.

meaningful plots of the solution has, in fact, been a significant task.) Again, numerical values shown on the plots are not important. Since the reaction takes place in a very narrow zone, the reaction-region structure is better exhibited, we believe, in Figures 5(a) and (5b).

In Fig. 5, the reaction rate at several times is contrasted for (a) unit stoichiometry ($\alpha = 1.0$) versus (b) non-unit stoichiometry ($\alpha = 0.5$). The reaction rate is plotted at a specified value of $\eta$, or radius, as a function of $\mu$, the coordinate normal to the flame front, for eight times in each case. Note that the reaction is skewed toward the fuel side for $\alpha = 0.5$ compared to the symmetric case of $\alpha = 1.0$.

Finally, in Fig. 6 is shown the result of plotting $Y_1/Y_{10} = Y_f/Y_{fo}$ and $Y_2/Y_{20} = Y_o/Y_{oo}$ versus $Z$ at many spatial points for three different times. At relatively early time, the concentration ratios for each species vary smoothly from zero to one with mostly fuel on the fuel side and mostly oxidizer on the other, but some of each on both sides of the reaction zone. At later times, however, the region of overlap where both fuel and oxidizer are nonzero decreases. Finally, at the last time, a state relation develops in which the relative concentrations depend only upon $Z$ and not on time, and fuel is only found to the left of the flame while only oxygen is found to the right. Also, the flame structure has collapsed to a flame sheet.

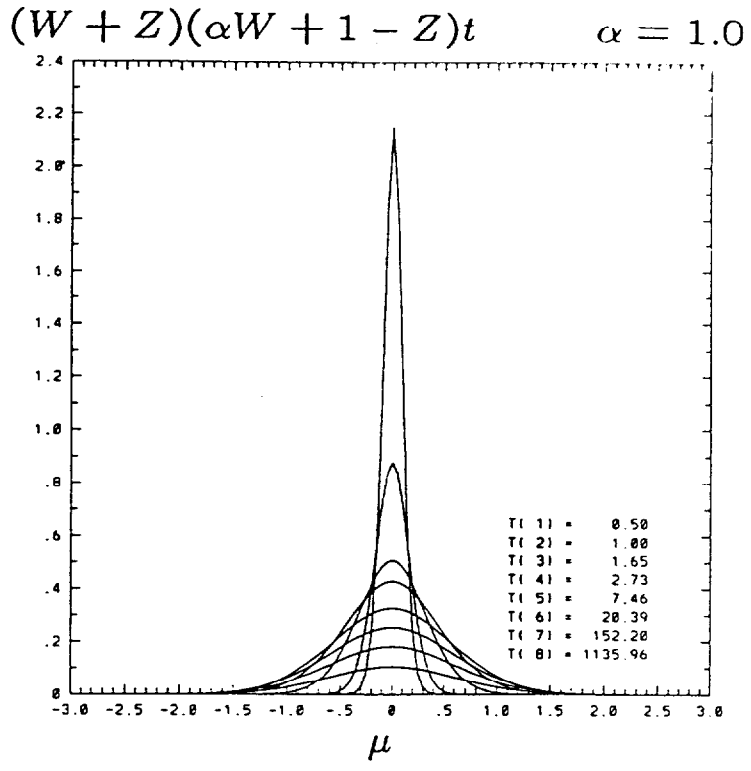


FIGURE 5 (a) Plots of the rate of reaction rate as a function of $\mu$, the coordinate normal to the flame front, for a fixed value of $\eta$, the radius, at eight times for $Re = 100$, $Sc = 10$ and $\alpha = 1$.

## 6 CONCLUSIONS

The analytical and computational results presented in this paper demonstrate several important features of a non-premixed flame, vortex interaction. First, we have introduced the pseudo-mixture-fraction variable together with a decomposition of the velocity field into a solenoidal component, determined by the imposed vortex, and an irrotational component, determined by the combustion heat release. The pseudo-mixture-fraction variable arises naturally as we transform the equations in the flame-sheet limit to account for variable transport properties and thermal expansion due to heat release. These transformations then reduce the governing equation to that of the constant-properties equation, allowing the solution to the latter problem to be interpreted in terms of the solution to the former problem. In particular, these transformations confirm in a detailed way the expected effect that thermal expansion has of pushing the flame-sheet away from the origin where the vortex resides. From the velocity-field decomposition, we also find an expression for the velocity potential generated by heat release and variable transport properties, see Eq. (8).

The model selected for the finite-rate process is one in which the gas phase reaction is for an isothermal, single-step, bimolecular reaction. As noted above, this model has been selected because unwanted fires are the primary area of interest of the authors,

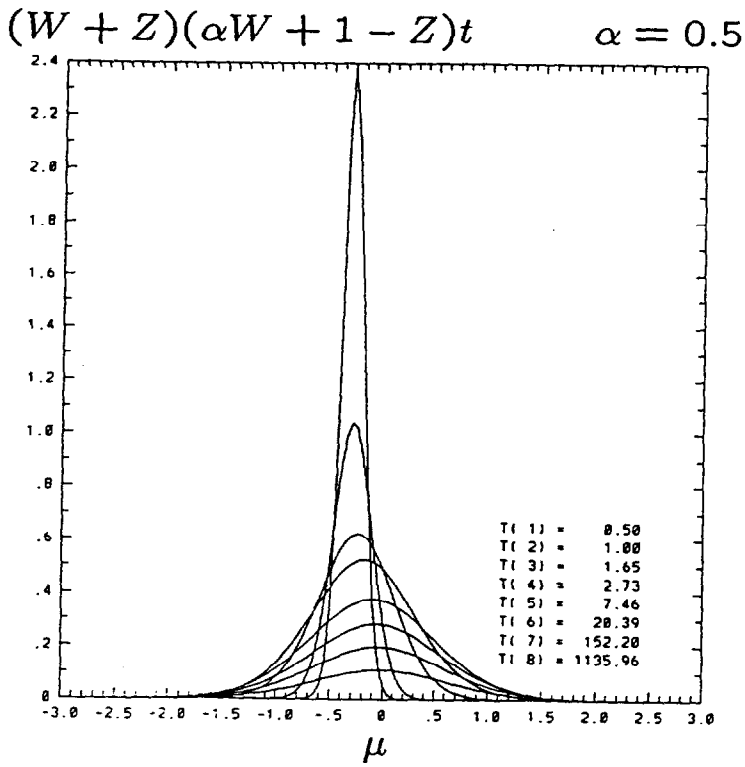


FIGURE 5 (b) Plots of the rate of reaction rate as a function of $\mu$, the coordinate normal to the flame front, for a fixed value of $\eta$, the radius, at eight times for $Re = 100$, $Sc = 10$ and $\alpha = 0.5$.

and in this context, it is expected that fuel has entered the gaseous state from a solid or liquid phase after pyrolyzation or evaporation by heat transfer from existing flames. The ignition of the fire is assumed in the unwanted fire and is not an issue. Only the ongoing combustion rate and its enhancement by mixing are of concern.

With a finite rate of reaction, a chemical kinetics time scale and a length scale derived from this time scale and the species diffusion coefficient are the appropriate scales with which to make the equations dimensionless. The dimensionless time then becomes a Damköhler number, as noted in Section 4. In unwanted fires, the long dimensionless time or large Damköhler number is the case of most practical importance. In this limit, the kinetics time scale becomes irrelevant and the analytical result of most interest is the similarity solution, or flame-sheet limit originally presented in Rehm et al. (1989) and revisited in Section 3 of the present paper. As observed in Rehm et al. (1989) and emphasized again here, that solution has no characteristic length nor time scale. We note here that similarity solutions are often of this nature, being solutions to which general, initial-value problems evolve as an intermediate asymptotic Barenblatt (1979).

A new and considerably simpler approximate asymptotic expression to this flame-sheet problem is also given in Section 3. The expression involves, of course, the error function in a coordinate normal to the flame sheet. This solution is of interest because it provides the correct normal coordinate in the large Schmidt number limit. Comparisons between

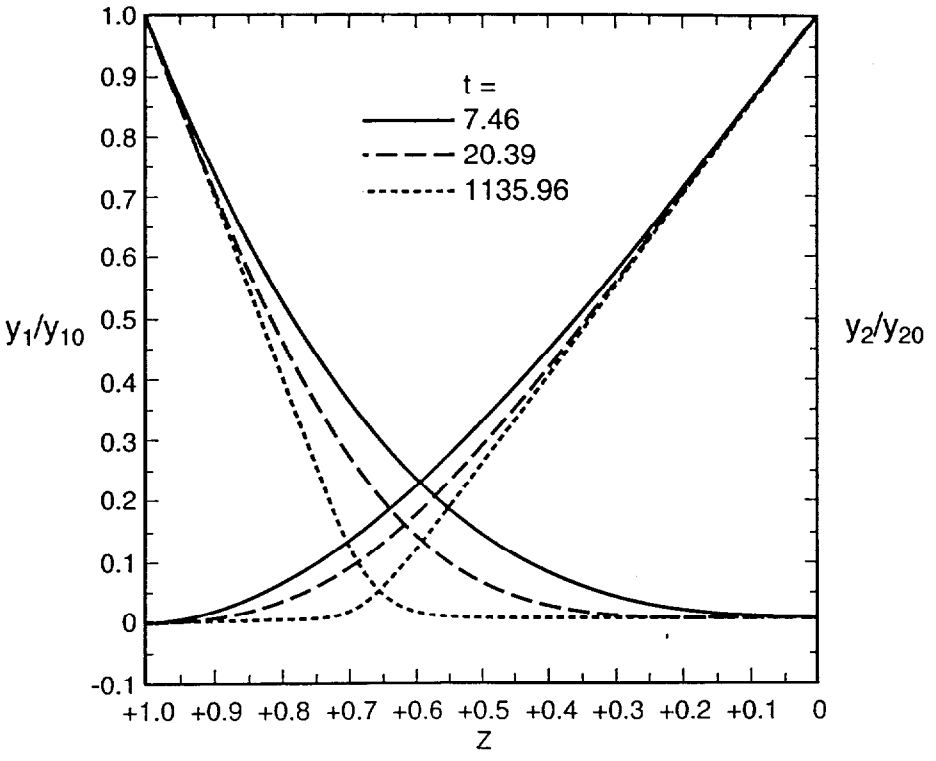


FIGURE 6 Plots of the variable $Y_1/Y_{10}$ and $Y_2/Y_{20}$ versus the mixture-fraction variable $Z$ at three different times. $t' = 7.5$, $20.4$ and 1136. The parameters for the plots are $Re = 100$, $Sc = 10$ and $\alpha = 0.5$.

this expression and the results obtained in Rehm et al. (1989) have been carried out. This solution, in conjunction with the analysis presented here and in Baum et al. (1991), is used to determine the first-order effects of thermal expansion and temperature-dependent transport properties. However, this solution also allows one to examine the structure of the reaction region when the Damköhler number is not large so that rate processes are important and to determine how the transition of the solution to the flame-sheet limit occurs. Results of calculations demonstrating the evolution of the reaction region are shown. Also, the evolution of the reaction to a state relation, dependent only upon the mixture-fraction variable, is demonstrated as the Damköhler number becomes large.

## 7 ACKNOWLEDGMENTS

The first author wishes to thank Professor John Ockendon and the Mathematical Institute of the University of Oxford for their hospitality during his visit in the Spring of 1989; part of this work was done at that time. R.G. Rehm is the corresponding author.

## REFERENCES

Barenblatt, G.I. (1979). *Similarity, Self-Similarity, and Intermediate Asymptotics*, Consultants Bureau, New York.

Baum, H.R., Corley, D.M. and Rehm, R.G. (1989). *Twenty First Symposium (International) on Combustion,* The Combustion Institute, 1263.

Baum, H.R., Rehm, R.G. and Gore, J.P. (1991). Transient combustion in a turbulent eddy. Twenty-Third Symposium (International) on Combustion, The Combustion Institute. 715.

Broadwell, J.E. and Breidenthal, R.E. (1982). A Simple Model of Mixing and Chemical Reaction in a Turbulent Shear Layer. *J. Fluid Mech.* **125.** 397.

Brown, G.L. and Roshko, A. (1974). On Density Effects and Large Structure in Turbulent Mixing Layers. *J. Fluid Mech.* **64,** 775.

Carrier, G.F., Fendell, F.E. and Marble, F.E. (1975). The effect of strain rate on diffusion flames. *SIAM J. Appl. Math.* **28** 453.

Cetegen, B.M., and Sirignano, W.A. (1990). Study of mixing and reaction in the field of a vortex. *Comb. Sci. Tech.* **72,** 157.

Cetegen, B.M., and Bogue, D.R. (1991). Combustion in a stretched fuel strip with finite rate chemistry, *Combustion and Flame* **86** 359.

Dahm, W.J.A., and Buch, K.A. (1989). High resolution three-dimensional ($256^3$) spatio-temporal measurements of the conserved scalar field in turbulent shear flows. University of Michigan, Department of Aerospace Engineering, Report No. GRI-5087-260-1443-4.

Friedlander, S.K., and Keller, K.H. (1963). *Chem. Engng. Sci.* **18,** 365.

Ghoniem, A.F., Heidarinejad, G. & Krishnan, A. (1988). On Mixing, Baroclinicity and the Effect of Strain in a Chemically-Reacting Shear Layer. Paper No. AIAA-88-0729, AIAA 26th Aerospace Sciences Meeting, Reno, Nevada.

Hermanson, J.C., Mungal, M.G. and Dimotakis, P.E. (1987). Heat Release Effects on Shear-Layer Growth and Entrainment. *AIAA Journal* **148,** 578.

Kapila, A.K. (1983). *Asymptotic Treatment of Chemically Reacting Systems,* Pitman Advanced Publishing Program, Boston, pp 77-91.

Karagozian, A.R. and Marble, F.E. (1986). Study of a diffusion flame in a stretched vortex. *Comb. Sci. Tech.* **45,** 65.

Karagozian, A.R. (1982). An analytical study of diffusion flames in vortex structures. Ph.D. Thesis, California Institute of Technology, Pasadena, Cal.

Karagozian, A.R. and Manda, B.V.S. (1986). Flame structure and fuel consumption in the field of a vortex pair. *Comb. Sci. Tech.* **49,** 185.

Laverdant, A.M. and Candel, S.M. (1988a). A numerical analysis of a diffusion-flame-vortex interaction. *Comb. Sci. Tech.* **60,** 79.

Laverdant, A.M. and Candel, S.M. (1988b). Etude do l'interaction de flammes de diffusion et de permelange aves un tourbillon. *La Recherche Aerospatiale* **3.** 13.

Laverdant, A.M. and Candel, S.M., (1989). Computation of diffusion and premixed flames rolled up in vortex structures. *J. Propulsion and Power* **5,** 134.

Macaraeg, M.G., Jackson, T.L. and Hussaini, M.Y. (1992). Ignition and structure of a laminar diffusion flame in the field of a vortex. *Comb. Sci. Tech.*.

Marble, F.E. (1985). Growth of a diffusion flame in the field of a vortex. Cassci, C. (Ed.), *Recent Advances in Aerospace Sciences* 315.

Meiburg, E. (1990). Lagrangian simulation of diffusion flames. *Comb. Sci. and Tech.* **71,** 1.

Mungal, M.G. and Dimotakis, P.E. (1984). Mixing and Combustion with Low Heat Release in a Turbulent Shear Layer. *J. Fluid Mech.* **148,** 349.

Mungal, M.G. and Frieler, C.E. (1988). The Effects of Damkohler Number in a Turbulent Shear Layer. *Combustion and Flame* **71.** 23.

Norton, O.P. (1983). The effects of a vortex field on flames with finite reaction rates. Ph.D. Thesis, California Institute of Technology, Pasadena, Cal.

Rehm, R.G., Baum, H.R., Lozier, D.W. and Aronson, J. (1989). Diffusion-controlled reaction in a vortex field. *Comb. Sci. Tech.* **66** 293.

Rehm, R.G., Baum, H.R., Tang, H.C. and Lozier, D.W. 1992. Finite-rate diffusion-controlled reaction in a vortex—a report. National Institute of Standards and Technology, Report NISTIR 4768.

Rogallo, R.S. and Moin, P. (1984). Numerical Simulations of Turbulent Flows. *Ann. Rev. Fluid Mech.* **16.** 99.

Son, S.F., McMurtry, P.A. and Queiroz (1991). The Effect of Heat Release on Various Statistical Properties of a Reacting Shear Layer. *Combust. and Flame* **85.** 51.

Williams, F.A. (1985). *Combustion Theory,* Second Edition, The Benjamin/Cummings Publishing Co., Menlo Park, CA.

Williams, F.A. (1985). Turbulent combustion. In Buckmaster, J.D. (Ed.), *The Mathematics of Combustion,* Frontiers in Mathematics, SIAM, Philadelphia, pp. 97-132.